ORIGINAL ARTICLE

WILEY

Postnatal ex vivo rat model for longitudinal bone growth investigations

Adamu Abdul Abubakar[1,2] (iD) | Sahar Mohammed Ibrahim[1,3] | Ahmed Khalaf Ali[1,3] |
Kareem Obayes Handool[1] | Mohammad Shuaib Khan[1,4] |
Mohamed Noordin Mustapha[5] | Tengku Azmi Ibrahim[6] | Ubedullah Kaka[7] |
Loqman Mohamad Yusof[1] (iD)

[1]Department of Companion Animal Medicine and Surgery, Universiti Putra Malaysia, Serdang, Malaysia

[2]Department of Veterinary Surgery and Radiology, Usmanu Danfodiyo University, Sokoto, Nigeria

[3]Department of Surgery and Theriogenology, College of Veterinary Medicine, University of Mosul, Mosul, Iraq

[4]Faculty of Veterinary and Animal Science, Gomal University, Dera Ismail Khan, Pakistan

[5]Department of Veterinary Pathology and Microbiology, Universiti Putra Malaysia, Serdang, Malaysia

[6]Department of Pre-Clinical Veterinary Sciences, Universiti Putra Malaysia, Serdang, Malaysia

[7]Laboratory of Sustainable Animal Production and Biodiversity, Institute of Tropical Agriculture and Food Security, Universiti Putra Malaysia, Serdang, Malaysia

Correspondence
Loqman Mohamad Yusof, Department of Companion Animal Medicine and Surgery, Universiti Putra Malaysia, Serdang, Malaysia.
Email: loqman@upm.edu.my

Funding information
Ministry of Higher Education Malaysia, Grant/Award Number: FRGS/1/2012/SGO5/UPM/02/9

Abstract

Background: Chondrocytes in the growth plate (GP) undergo increases in volume during different cascades of cell differentiation during longitudinal bone growth. The volume increase is reported to be the most significant variable in understanding the mechanism of long bone growth.

Methods: Forty-five postnatal Sprague-Dawley rat pups, 7-15 days old were divided into nine age groups (P7-P15). Five pups were allocated to each group. The rats were sacrificed and tibia and metatarsal bones were harvested. Bone lengths were measured after 0, 24, 48, and 72 hours of ex vivo incubation. Histology of bones was carried out, and GP lengths and chondrocyte densities were determined.

Results: There were significant differences in bone length among the age groups after 0 and 72 hours of incubation. Histological sectioning was possible in metatarsal bone from all age groups, and in tibia from 7- to 13-day-old rats. No significant differences in tibia and metatarsal GP lengths were seen among different age groups at 0 and 72 hours of incubation. Significant differences in chondrocyte densities along the epiphyseal GP of the bones between 0 and 72 hours of incubation were observed in most of the age groups.

Conclusion: Ex vivo growth of tibia and metatarsal bones of rats aged 7-15 days old is possible, with percentage growth rates of 23.87 ± 0.80% and 40.38 ± 0.95% measured in tibia and metatarsal bone, respectively. Histological sectioning of bones was carried out without the need for decalcification in P7-P13 tibia and P7-P15 metatarsal bone. Increases in chondrocyte density along the GP influence overall bone elongation.

KEYWORDS

bone growth model, chondrocytes, endochondral ossification, growth plate, Sprague-Dawley rat

---

1 | INTRODUCTION

The mammalian growth plate (GP) is an important region of long bone that directly mediates and regulates longitudinal bone growth. Longitudinal bone growth occurs through a series of cellular differentiation stages at the epiphyseal GP region.[1,2] The whole process begins with condensation of the chondro-proginator cells at the resting zone. The chondro-proginator cells differentiate, mature and become round chondrocytes. The round chondrocytes become flattened, proliferate and are then organized into columns.[3] The proliferative chondrocytes then cease to divide and differentiate into prehypertrophic chondrocytes (PHCs) before undergoing a significant increase in cell volume of about 20-fold to become hypertrophic chondrocytes (HCs).[4,5] The HCs are considered to be specialized cells that signify the end-state of the chondrocyte differentiation pathway, and play a crucial role during endochondral ossification.[6] The mature HCs release matrix vesicles that initiate cartilage calcification and perichondrial cell differentiation into osteoblasts, and secrete bone extracellular matrix (ECM), which surrounds the hypertrophic zone and is organized into a periosteum that later produces the diaphyseal shaft of the long bone.[7]

Previous studies involving bone growth and development for mammalian applications utilized embryonic bone from rats at different gestation periods and bone from postnatal rats mostly aged 7 days (P7).[5,8–10] In those studies, the investigators' hypothesis was that embryonic bones can be cultured ex vivo for longer than a day without deteriorating, while postnatal bone cannot be cultured for more than 24 hours in conventional ex vivo bone culture medium if optimal bone growth rate is to be sustained. It was also thought that bone growth rates are maximal in embryonic and P7 rats, because, as previously reported,[11,12] up to P7 bone is considered to be metabolically active and the bones can easily be sectioned for histology without the need for decalcification in order to maintain in situ bone morphology and structures. However, the use of embryonic and P7 bone models has been reported to present challenges in terms of bone handling and manipulation, even when using a dissecting stereo microscope. The relatively small size of the bones and their fragility makes it difficult to harvest the bones and to free the surrounding soft tissue from the bone without affecting the bone periosteum and the epiphyseal growth plate (EGP).[11]

Ex vivo culture of bone could be useful in investigations of the various parameters of endochondral bone formation such as bone growth rate, metabolic activity and other vital parameters of interest that can be determined using standard experimental procedures described by numerous investigators and available image analysis software.[13] Histomorphological in situ hybridization and immunohistological staining using specific primary antibodies of interest may be readily performed on the cultured bone sections, which will allow a wider exploration of both cellular and molecular entities during endochondral bone formation, thus providing a major advantage over the conventional in vitro cell culture approach.[13] Another major advantage of the ex vivo bone culture model is the elimination of systemic factors that may influence bone growth when tested in an in vivo environment.[10] In addition to these advantages, a successful ex vivo model could also provide a means of avoiding unnecessary utilization of live animals and encourage replacement of live animal for experimental purposes.

In order to gain further detailed insights into ex vivo mammalian endochondral bone growth, a postnatal rat model that can offer an optimal growth pattern is required. It is equally important to have a postnatal bone model that can be histologically sectioned without the need for decalcification. We hypothesized that the long bones of rats aging between 7 and 15 days old is suitable for ex vivo longitudinal bone growth study and shows optimal growth rates within 72 hours of culture. The aim of the study was to measure and compare the postnatal ex vivo growth patterns of tibia and metatarsal bones using a postnatal rat model with an age range of 7-15 days, and to determine the feasibility of the postnatal bone for histological sectioning without the need for decalcification. To achieve this, the ex vivo longitudinal growth rate pattern of the two long bones (tibia and metatarsal bone), the ease of histological sectioning, and the GP length and chondrocyte density in different zones based on the histological sections, were determined.

2 | MATERIALS AND METHODS

2.1 | Culture medium and biochemical solutions

The bone dissection medium consisted of phosphate buffered saline (PBS; Fisher bioReagent®, USA) containing 7.5% v/v α-modified essential medium (α-MEM; Naclai Fesque Inc. Tokyo, Japan), 10% w/v fetal bovine serum (FBS; Naclai Fesque Inc. Tokyo, Japan) at pH 7.4. The standard bone culture medium used was α-MEM supplemented with 1 mmol/L sodium glycerol biphosphate powder (Sigma-Aldrich, USA), 5 mg/mL L-ascobic acid powder (Fisher Scientific, UK), and penicillin-streptomycin antibiotic (Sigma-Aldrich, USA) at a final concentration of 100 IU/mL and 100 μg/mL, respectively. Bone samples for histological sectioning were fixed in 4% paraformaldehyde (Acros Organics, New Jersey, USA). Slides were stained with 0.1% toluidine blue O, in PBS at pH 5.6, and von Kossa stain (Acros Organics, New Jersey, USA). The FBS used in this study was inactivated as described by Rahman et al.[14] The inactivation was achieved using gradual heating in a water bath at 56°C for 30 minutes prior to incorporation into the α-MEM media.

2.2 | Animal preparation

Forty-five Sprague-Dawley rat pups aged 7-15 days (P7-P15) were used in this study. The pups were randomly divided into nine age groups with five rats per group (n = 5). The rats were humanely sacrificed using 20% pentobarbital (Dolethal®; Vetoquinol, France) at 90 mg/kg following Universiti Putra Malaysia Institutional Animal Care and Use Committee approval (Reference no. R028/2015). The left and right tibia and corresponding three middle metatarsals of

each limb were carefully dissected, along with proximal and distal epiphyseal growth plate cartilages, using a dissecting stereo-microscope (Huvitz; HSZ-645TR, Korea). In each group, 10 tibia and 30 metatarsal bones were successfully harvested. The dissected limbs were temporarily placed in dissecting medium containing PBS, 7.5% v/v α-MEM, and 1 mmol/L FBS at pH 7.4 in order to maintain bone viability prior to incubation.

Preparation of dissecting media and standard bone culture media, tissue dissections and culture work were all performed in a laminar flow hood to ensure the sterility of the media and the harvested bones. The culture and dissection media were allowed to equilibrate for at least 1 hour in a 5% CO_2 incubator at 37°C prior to use, as previously reported.[13] The dissection instruments were autoclaved and immersed in 70% ethanol prior to use to avoid contamination. The dissecting and standard bone culture media were filter sterilized through a 0.22 μm, 33 mm diameter syringe filter.

2.3 | Tibial and metatarsal length measurements

Digital images of the long bones were captured at 0, 24, 48, and 72 hours of incubation and the length was measured from the proximal to distal end. The length of the harvested tibia and metatarsal rudiments from different age groups (P7-P15) were measured with VIS plus ver.3.50 image analysis and measurement software (Canada). The dissecting stereo-microscope was fitted to a 3.1 mega pixel digital camera (VIS imaging; UC3010; Malaysia) connected to a PC via USB cable. The lengths of the bones were measured in centimeters (cm) at ×6.5 magnification. Images were analyzed as previously described.[15] The overall bone length was measured before incubation at baseline, and subsequently at 24, 48, and 72 hours of incubation. The bone growth rate was expressed as a percentage bone length increase at every 24 hours from the baseline length measured before incubation (0 hour).

The tibial bones from the different age groups (P7-P15) were cultured individually in a 6-well tissue culture plate (flat bottom cell culture plate with lid; Sigma-Aldrich, USA), while the metatarsal bone rudiments were cultured individually in a 24-well cell culture plate (Nuclon™, delta surface, China). The bones were incubated for periods of 24, 48, and 72 hours in the standard culture medium described earlier at (5% CO_2, 95% air, pH 7.4, and 37°C). The medium was discarded after every 24 hour incubation period, and at each change of medium, a minimum of five tibias and ten metatarsal bone rudiments were randomly selected for histological processing.

2.4 | Preparation of growth plate for histology

Bones were fixed overnight in 4% paraformaldehyde at pH 7.4 to avoid previously reported fixative-induced artifacts to chondrocyte shape and volume.[11] The bones were then dehydrated in a series of ethanol solutions using a TP 1020 semi-closed bench top tissue processor (Leica, Singapore). The bones were then embedded in paraffin wax using standard procedures.[16] Samples were then serially sectioned longitudinally into 4-5 μm thick sections using a Reichert-Jung 2045 multicut rotary microtome (USA). The sections were finally mounted on poly-L-lysine coated microscope slides (Menzel-Glaser, Germany). After de-parafinization with xylene and rehydration with decreasing concentrations of ethanol solution (100% and 70%), the sections were stained with 0.1% toluidine blue O in PBS (pH 5.6, 30 seconds, 23°C) and von Kossa stain, using a technique adapted from Pastoureau et al and Schmitz et al.[17,18]

2.5 | Quantitative histology

Histologic images of the proximal EGPs were captured using an inverted fluorescence microscope (Nikon Eclipse Ti-S, Japan) fitted with a 10 × (numeric aperture = 0.5WD [82 000 μm]) dry objective lens. In order to determine the beginning and terminal end of the EGPs several subjective criteria were used based on cell size and organization, as described previously by Alvarez et al and Wilsman et al.[19,20] The EGP length and its different zones were identified and measured using an established procedure described by Bush et al.[21] The potential secondary ossification center and articular cartilage surface were not included in the measured area of the growth plate. Briefly, the zones of the EGP were identified manually by eye and marked by drawing a freehand line. The histologic zones identified were: the resting zone at the top of proliferating cell border, the proliferating chondrocyte zone, the early and late hypertrophic chondrocyte zones, and the mineralized region within the hypertrophic zone. Chondrocytes were considered to be early hypertrophic when their size was less than or equal to 7 μm, compared to late hypertrophic chondrocytes which were greater than 7 μm of size. In addition, the early hypertrophic chondrocytes were fully nucleated, while most of the late hypertrophic chondrocytes were anucleated because of apoptosis or autophagy-induced changes.[6,22] Furthermore, the hypertrophic chondrocytes were defined as having a height range of 7-13.48 μm. The late hypertrophic chondrocytes were further defined as the cells in the last lacuna that were not invaded by metaphyseal blood vessels, as described by Waise et al, Tivesten et al, Amini et al, and Chagin et al.[8,23–25] The total length of the proximal EGP and the total EGP chondrocyte density in the proliferative and hypertrophic zones were measured and counted. The measurement was performed using NIS-Element BR4.20.00 64-bit analytical software (Nikon, Japan) fitted with a Nikon digital sight camera DS-Fi2, K16850 (Nikon Corporation, Japan). Prior to the image capture, the micrograph images of the EGP were aligned so that the direction of growth was vertical on the computer screen. The height of the entire EGP and the heights of the separate growth zones were obtained by demarcating the EGP from the top resting zone. The junctions between resting and proliferative zones and between proliferative and hypertrophic zones were outlined based on the morphological characteristic of the chondrocytes stated earlier, as well as the changes in the histological matrix staining.[26] The vertical height of the total EGP was then measured at five different locations per section as described by Wilsman et al.[20] The total chondrocyte cell density was determined based on the total cell numbers counted over at least three measured areas of interest (cells/mm^2) per slide.

2.6 | Data analysis

Data were presented in the form of tables and graphs. Comparison between two sets of data was done by Student's t test or a suitable non-parametric test if the data sets were not normally distributed. Time course experiments were analyzed with a repeated measure two-way ANOVA for which appropriate post hoc tests for multiple comparisons were conducted. Analysis was carried out using IBM SPSS for windows, version 22.0, while graphs were plotted using GraphPad Prism 7. Data are presented as mean and standard error of the mean (SEM). $P < 0.05$ were considered significant.

3 | RESULTS

3.1 | Tibial and metatarsal epiphyseal growth rates

Tibial and metatarsal lengths were measured at 0, 24, 48, and 72 hours of incubation as previously described in Materials and Methods (Figure 1). There was a significant increase in tibial length across all the age groups and incubation periods. Two-way ANOVA revealed significant differences in tibial bone lengthening among all the age groups at three incubation times (Table 1). Maximum growth was recorded from tibial bone from the P10 age group at 48 and 72 hours of incubation (2.75 ± 0.14 cm and 2.8 ± 0.07 cm, respectively) (Table 1). Tibial lengthening significantly differed among the three incubation time in all the age groups. Significant differences were recorded between 0, 24, and 48 hours of incubation. The difference in lengths recorded between 48 and 72 hours of incubation was not significant in most of the age groups.

The percentage increase in tibial and metatarsal lengths was higher between the 24 and 48 hours incubation periods than between the 48 and 72 hours incubation periods in every individual age group (Figures 2 and 3). There was significant percentage growth of both tibia and metatarsal bones between 24 and
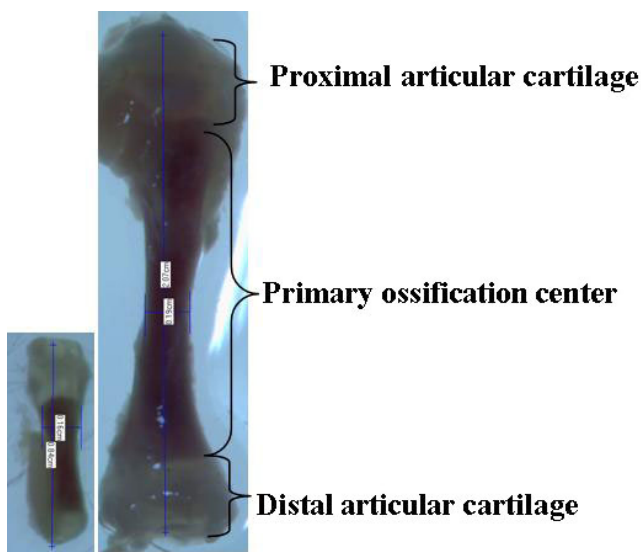
48 hours of incubation and between 24 and 72 hours of incubation across all age groups. However, there was no significant percentage bone growth between 48 and 72 hours of incubation in almost all the age groups (Figures 2 and 3). The lowest tibial growth rate (10 ± 1.6%) was observed in the 13-day-old age group (P13) after 72 hours of incubation. On the other hand, the highest tibial growth rate was observed in the P10 age group during the 48 and 72 hours incubation periods (26 ± 1.4% and 29 ± 1.5%, respectively) (Figure 3). The lowest metatarsal growth rate (17.2 ± 1.4%) was observed in the 9-day-old age group after 24 hours of incubation, while the highest metatarsal growth rate (47.9 ± 1.4%) was observed in the P12 and P13 age groups during the 72 hours incubation period (Figure 3).

The significant differences in metatarsal growth length recorded among all the age groups at different incubation periods were similar to those of the tibia bone. There was a significant difference in metatarsal lengthening among the age groups at three different incubation periods. The highest metatarsal bone lengthening was observed in the 15-day-old age group at 24, 48, and 72 hours of incubation (1.5 ± 0.1 cm, 1.61 ± 0.11 cm, and 1.66 ± 0.1 cm, respectively) (Table 2). There was a trend towards a progressive increase in total metatarsal and tibial bone lengths from baseline with the increasing age amongst the P7-P15 age groups.

The overall percentage tibial and metatarsal growth rates recorded across the age groups after 72 hours of incubation period were 23.87 ± 0.80% and 40.38 ± 0.95%, respectively. There was a significant difference between the percentage growth rates of the two bones under investigation (Table 3).

3.2 | Histological sectioning of the whole bones

Histological sectioning of tibia without decalcification was possible across all the first seven age groups (P7-P13), representing 77.8% of the total age groups studied. Sectioning of the remaining age groups (P14 and P15) was possible, but with slight additional difficulties. On the other hand, metatarsal sectioning was possible across all the age groups without the need for a decalcification process (Figure 4).

3.3 | Total epiphyseal growth plate (EGP) length

Total proximal EGP lengths of tibia and metatarsal bones were measured at 0 and 72 hours as described in Materials and Methods (Figure 5). There were significant differences ($P < 0.005$) in total EGP lengths of tibia among the respective age groups at each 0 and 72 hours incubation. However, there were no significant differences in the total tibial EGP lengths between 0 and 72 hours except in the P12 and P15 age groups (Table 4).

There were also significant differences ($P < 0.05$) in metatarsal total EGP length among the age groups at each 0 and 72 hours of incubation (Table 4). However, there was no significant difference in the total metatarsal EGP length between 0 and 72 hours of incubation in all age groups under investigation.

FIGURE 1 Metatarsal and tibial bone length measurement

Proximal articular cartilage

Primary ossification center

Distal articular cartilage

TABLE 1 Tibial length (cm) among all the age groups after different incubation periods

Age group (d)	0 h (n = 10)	24 h (n = 10)	48 h (n = 7)	72 h (n = 4)
P7	1.42 ± 0.13[a,x]	1.55 ± 0.14[a,x]	1.59 ± 0.01[a,x]	1.68 ± 0.11[a,x]
P8	1.72 ± 0.21[c,x]	1.88 ± 0.02[b,y]	1.89 ± 0.20[b,z]	1.88 ± 0.22[b,z]
P9	1.77 ± 0.13[b,x]	2.10 ± 0.13[c,y]	2.38 ± 0.11[c,z]	2.56 ± 0.01[c,z]
P10	2.08 ± 0.08[d,x]	2.46 ± 0.08[d,y]	2.75 ± 0.14[d,z]	2.8 ± 0.007[d,e,z]
P11	2.16 ± 0.12[d,e,x]	2.52 ± 0.00[d,e,y]	2.60 ± 0.01[d,e,z]	2.64 ± 0.06[d,e,z]
P12	2.21 ± 0.10[d,e,x]	2.47 ± 0.04[d,e,y]	2.63 ± 0.04[f,z]	2.67 ± 0.01 [g,z]
P13	2.24 ± 0.11[d,e,f,x]	2.29 ± 0.09[d,y]	2.55 ± 0.10[d,z]	2.58 ± 0.01[d,e,z]
P14	2.28 ± 0.10[e,f,x]	2.48 ± 0.21[d,y]	2.55 ± 0.10[d,e,z]	2.59 ± 0.02[f,z]
P15	2.40 ± 0.12[f,x]	2.57 ± 0.05[e,y]	2.61 ± 0.00[d,e,f,z]	2.65 ± 0.09[f,g,z]

Data were expressed as means ± SEM.
[x,y,z]Significant differences in mean tibial length between the incubation times in each age group.
[a,b,c,d,e,f]Significant differences in mean tibial length between the age groups at different incubation times ($P < 0.05$; two-way ANOVA).
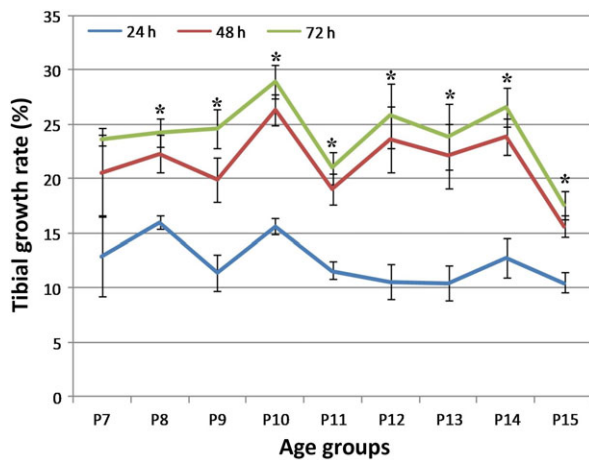

FIGURE 2 The graph shows percentage tibial growth rates in different age groups after incubation for different periods (24, 48, and 72 hrs). Each data point represents mean growth rate (%) of 5 tibias (n = 5) for different incubation periods. Data were expressed as means ± SEM. *Significant differences ($P < 0.05$; one-way ANOVA) in tibial growth rate between the incubation periods of each age group

FIGURE 3 The graph shows percentage metatarsal growth rates in different age groups after incubation for different periods (24, 48, and 72 hrs). Each data point represents the mean of 10 metatarsals (n = 10). The growth rate was determined based on the changes in the metatarsal lengthening during different incubation periods and was expressed as a percentage increase from the baseline length. Data were expressed as means ± SEM. *Significant differences ($P < 0.05$; one-way ANOVA) in metatarsal growth rate between the incubation periods of each age group

3.4 | Epiphyseal growth plate chondrocyte (EGPC) density

Proximal tibial and metatarsal EGPC density was determined in all the age groups at 0 and 72 hours of incubation, as described in Materials and Methods. There was an apparent trend towards an increase in total chondrocytes density along the entire EGP of both metatarsal and tibia bones among all age groups (P7-P15) from baseline to 72 hours of incubation. However, there were no significant differences in the EGPC densities among the age groups at both baseline and 72 hours of incubation ($P > 0.05$; two-way ANOVA). On the other hand, there was also a trend towards an increase in EGPC densities in both metatarsal bones and tibia from the baseline to 72 hours of incubation in all the groups. Similarly, there were significant differences in EGPC
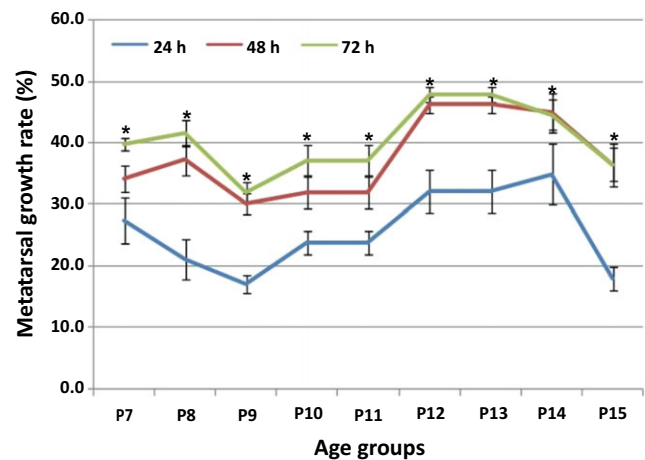
densities ($P < 0.05$) between the 0 and 72 hours incubation periods in all the age groups except in the tibial P13, P14 and P15 age groups. The metatarsal P11, P12, P14 and P15 age groups also show no significant differences between the 0 and 72 hours incubation periods in EGPC densities (Table 5). There were no significant differences in total metatarsal EGP chondrocyte density among the age groups at both 0 and 72 hourss.

4 | DISCUSSION

One of the limitations of this study was that only proximal EGP was used for histological assessment of the parameters. The choice of the

TABLE 2 Metatarsal length (cm) among all age groups after different incubation periods

Age group (d)	0 h (n = 30)	24 h (n = 30)	48 h (n = 20)	72 h (n = 20)
P7	0.54 ± 0.10[a,x]	0.67 ± 0.09[a,y]	0.74 ± 0.11[a,z]	0.75 ± 0.11[a,z]
P8	0.56 ± 0.10[a,x]	0.66 ± 0.07[a,y]	0.68 ± .010[b,z]	0.72 ± 0.14[a,z]
P9	0.85 ± 0.22[b,x]	1.05 ± 0.12[b,y]	1.20 ± 0.11[c,z]	1.25 ± 0.10[b,z]
P10	0.93 ± 0.11[b,x]	1.25 ± 0.14[c,y]	1.40 ± 0.09[c,d,z]	1.45 ± 0.08[b,c,z]
P11	1.00 ± 0.10[b,x]	1.07 ± 0.14[c,y]	1.14 ± 0.13[c,d,z]	1.18 ± 0.08[c,d,z]
P12	1.01 ± 0.17[b,x]	1.21 ± 0.11 [g,y]	1.25 ± 0.10[f,z]	1.26 ± 0.06[d,e,z]
P13	1.01 ± 0.11[b,c,x]	1.15 ± 0.05[e,f,y]	1.19 ± 0.11[e,z]	1.20 ± 0.49[e,z]
P14	1.10 ± 0.10[c,d,x]	1.18 ± 0.09[c,e,y]	1.22 ± 0.12[d,e,z]	1.29 ± 0.14[c,d,z]
P15	1.22 ± 0.13[d,x]	1.50 ± 0.10 [g,y]	1.61 ± 0.11[f,z]	1.66 ± 0.10[e,z]

Data were expressed as means ± SEM.
[x,y,z]Significant differences in mean metatarsal length between the incubation times in each age group.
[a,b,c,d,e,f]Significant differences in mean tibial length between the age groups at different incubation times ($P < 0.05$; two-way ANOVA).

TABLE 3 Overall tibial and metatarsal percentage growth rate after 72 hrs of incubation

Bone type	Overall mean growth rate	N	P value
Tibia	23.87 ± 0.81	n = 64	0.009
Metatarsal	40.38 ± 0.99	n = 87	

proximal over the distal region was based on the adapted experimental protocol described by Loqman et al and Dobie et al.[11,27] There could be growth variation between the proximal and distal EGP of the long bones. Longitudinal bone growth in mammals is primarily achieved through chondrogenesis mediated by chondrocytes mainly in the proliferative and hypertrophic zones of the EGP.[5] The complete time cycle of chondrocyte differentiation and maturation leading to bone elongation via endochondral ossification occurs within approximately 24 hours in rapidly growing mammals.[28–32] The stages of chondrogenesis occur in a highly coordinated manner,[33,34] within the three distinct zones of the EGP. Proliferation of chondrocytes, their enlargement during hypertrophy, and extracellular matrix synthesis are the most important process in long bone growth.[6,35,36]

This study demonstrates that postnatal tibia and metatarsal bone rudiments from rats 7-15 days old can be experimentally cultured for up to 72 hours and maintain remarkable increases in length. These results contrast with previous reports from investigators such as Marino et al,[12] who assumed that postnatal conventional ex vivo bone growth above 24 hours incubation is slow. The marked ex vivo increase in bone length within the 72 hours culture period suggests there is rapid proliferation and maturation of chondrocytes during early postnatal life, as reported by Crombrugghe et al, Farnum et al, and von Pfeil and DeCamp.[36–38] The significant differences in tibial and metatarsal growth rates observed among the age groups under investigation is a strong indication that early postnatal growth rate of long bones is age dependent, and bone growth in rats is active during postnatal days 7-15. Nilsson and Baron[39] reported that long bone growth occurs rapidly in early postnatal life then slows and subsequently ceases. According to their findings, the decline in growth rate is mainly due to a decrease in the morphological changes in EGP cartilage during postnatal development.

Our finding of significant growth differences among the tibial age groups concurs with that of Wilsman et al,[20] who reported significant growth variation among tibial bones among different age groups of rats. Alvarez et al[19] reported that different growth rates of tibia are associated with changes in the expression pattern of type II and X collagen and collagenase 3 at the proximal GP in rats.

The maximum growth rate among age groups in our study was recorded in 10-day-old tibia after 72 hours of incubation, which indicates that tibia from P10 rats can produce the optimal bone growth rate in ex vivo rat bone growth model. The significant differences in tibial and metatarsal percentage growth rates recorded during different incubation periods (24, 48, and 72 hourss) strongly suggests that ex vivo early postnatal bone growth rates vary among different age groups. This finding also indicates that EGP chondrocytes remain viable and can be physiologically active up to 72 hours after the rat has been sacrificed, if cultured in appropriate physiological conditions. Further investigation may be required to ascertain the percentage viability of the chondrocytes throughout the 72 hours duration of incubation. It was observed that metatarsal bone rudiments have a higher percentage growth rate in comparison with tibia, which could be associated with a more frequent hypertrophic chondrocyte turnover within a 24 hours cycle in metatarsal bone compared with tibia, as reported by Cooper et al.[40] The higher percentage growth rate observed in metatarsal bone could also be related to its higher non-mineralized trabecular bone component; Abubakar et al and Mohammed et al[10,41] reported that trabecular bones are more metabolically active that the cortical component due to high osteogenic activity within the cancellous component of the bone.

Histological sectioning of the tibia of the P7-P13 rats and all the metatarsal rudiments was easily carried out, which suggested that active tibial mineralization commences at postnatal day 14. In the case of metatarsal rudiments, the exact day on which active mineralization commences is not known since all the metatarsal bones from all the age groups (P7-P15) under investigation were sectioned successfully without any difficulty. Further investigation is needed to quantify the postnatal degree of long bone mineralization to ascertain the exact period of active metatarsal bone mineralization.
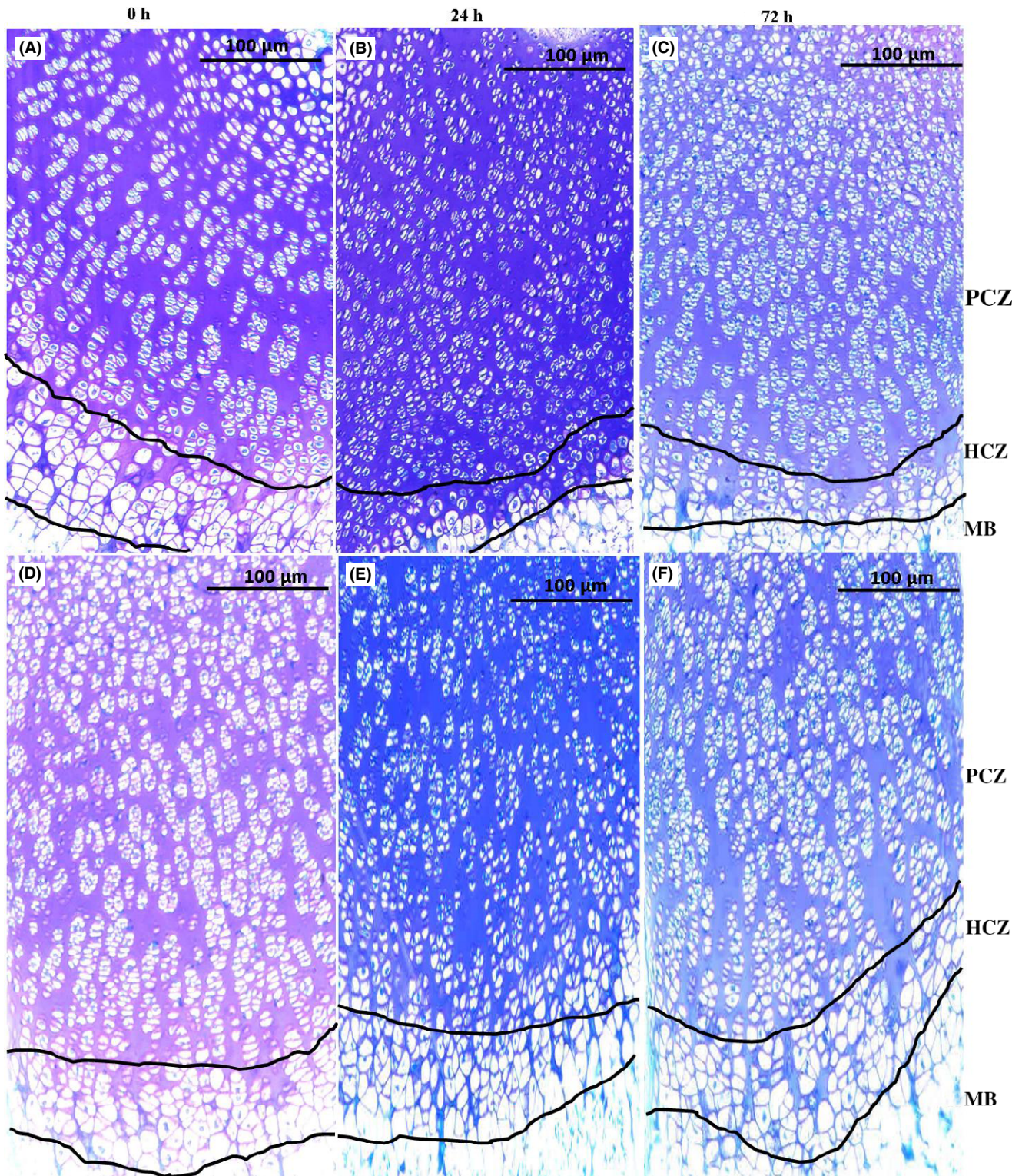
FIGURE 4 Representative histomicrograph images of the proximal EGP of tibial (A-C) and metatarsal (D-F) shows EGP length and chondrocyte density. A, B, and C, tibia EGP of P10 rats at 0, 24 and 72 h, respectively, of incubation. D, E, and F, metatarsal EGP at the different incubation periods, indicating cellular differences at different zones of the EGP. PCZ, proliferative chondrocyte zone; HCZ, hypertrophic chondrocyte zone; MB, mineralized bone. The zones of the GP are demarcated by the two black lines. Images were captured using a ×10 objective; scale bar = 100 μmol/L in all panels. Slides were stained with toluidine blue O

The significant differences in total EGP length in both tibia and metatarsal bone among the age groups at baseline and after 72 hours of incubation suggests that the total EGP length of the rats varied with age. The result also suggests that the optimal length of total EGP in the tibia and metatarsal bone model was achieved in P10 age group before it declined in older age groups. This finding

concurs with previous findings reported by Martin et al and Nilsson and Baron that the epiphyseal GP regresses over time before it closes completely.[39,42] It should be noted that rats are exceptional in this respect, as their epiphyseal GPs do not close completely during their life time but progressively diminish over time.[43,44] The gradual fusion of the growth plate in mammals is reported to occur by means of a decrease in chondrocyte proliferation and differentiation along the entire EGP.[39] On the other hand, we observed that no significant differences in total EGP length between the baseline and 72 hours of incubation in either tibia or metatarsal bones. This suggests that the EGP length is not a major determinant of longitudinal bone growth by means of endochondral ossification; a similar finding was also reported by Wilsman et al.[45] Although significant bone lengthening was achieved over the 72 hours incubation period, this could be influenced by other aspects of the EGP apart from its total length. Apart from the direct contribution of chondrocyte proliferation and differentiation in the EGP, there are numerous local and systemic factors that have been reported to significantly influenced bone growth both in vivo and ex vivo.[5,46-48] Growth hormone (GH), among other factors, is one of the major systemic regulators of longitudinal bone growth. GH function appears to be linked to production of IGF-1, which is reported to be a major contributor to stimulation of colonal expression of proliferating chondrocytes in the EGP region leading to bone elongation.[48] One of the limitations of this ex vivo bone growth model is the possible influence of external stimulation with IGF-1 on linear bone growth that was not investigated.

This study also revealed significant variation in total EGP chondrocytes between the 0 and 72 hours incubation periods in most
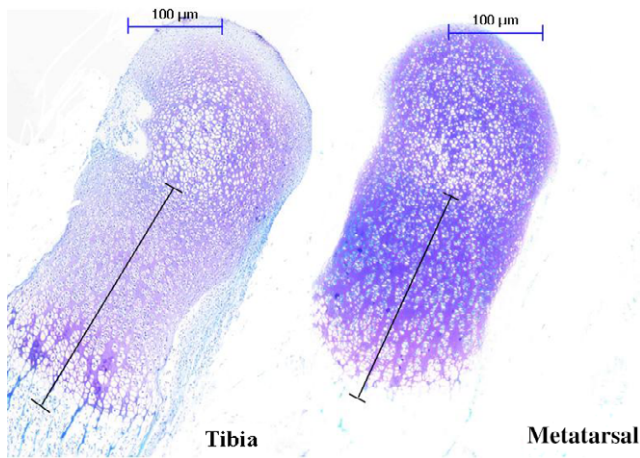

FIGURE 5 Metatarsal and tibial epiphyseal growth plate length measurement. Length of the EGP excluding the potential secondary ossification centers and the articular surface cartilage. Images were captured using a ×4 objective; scale bar = 100 μmol/L in all panels. Slides were stained with toluidine blue O

TABLE 5 Tibial and metatarsal GPC density (cells/mm^2) at 0 and 72 h of incubation

Age group (d)	Tibial GPC density (cells/mm^2)		Metatarsal GPC density (cells/mm^2)	
	0 h (n = 5)	72 h (n = 5)	0 h (n = 5)	72 h (n = 5)
P7	3173 ± 5^x	3910 ± 8^y	2851 ± 7^x	3069 ± 7^y
P8	3188 ± 5^x	3913 ± 162^y	2889 ± 151^x	3082 ± 90^y
P9	3224 ± 21^x	3950 ± 269^y	2910 ± 167^x	3092 ± 222^y
P10	3253 ± 24^x	3951 ± 333^y	2962 ± 26^x	3098 ± 357^y
P11	3312 ± 35^x	3962 ± 456^y	3004 ± 376^x	3107 ± 414^x
P12	3314 ± 41^x	3969 ± 535^y	3014 ± 324^x	3157 ± 406^x
P13	3316 ± 47^x	3965 ± 616^x	3033 ± 230^x	3159 ± 362^x
P14	3311 ± 247^x	3932 ± 330^x	3061 ± 111^x	3150 ± 270^x
P15	3354 ± 131^x	3938 ± 453^x	3096 ± 185^x	3145 ± 306^x

Data were expressed as means ± SEM.
^{x,y}Significant differences in total tibial GP chondrocytes density between 0 and 72 h of incubation time in each age group ($P < 0.05$; two-way ANOVA). There were no significant differences in total GP density among the age groups.

TABLE 4 Total proximal tibial and metatarsal EGP length (μm) at 0 and 72 h of incubation

Age group (d)	Proximal tibia GP length (μm)		Proximal metatarsal GP length (μm)	
	0 h (n = 10)	72 h (n = 10)	0 h (n = 10)	72 h (n = 10)
P7	550.20 ± 86.29^a	555.20 ± 84.81^a	496.40 ± 85.60^a	551.90 ± 87.29^a
P8	611.00 ± 120.27^{a,b}	643.50 ± 111.48^{a,b}	570.50 ± 113.89^a	639.50 ± 105.62^b
P9	956.90 ± 85.01^{a,b,c}	1115.40 ± 106.69^{a,b,c}	1175.10 ± 109.74^c	1200.60 ± 99.80^a
P10	1280.90 ± 178.04^c	1548.00 ± 201.18^c	1155.90 ± 120.58^c	1237.10 ± 107.55^c
P11	1126.00 ± 138.04^{b,c}	1353.50 ± 194.15^c	1077.90 ± 130.32^{b,c}	1156.90 ± 115.77^d
P12	952.00 ± 50.47^{a,b,c,x}	1305.00 ± 191.88^{b,c,y}	932.80 ± 41.13^{a,b,c}	1020.50 ± 41.14^{e,x}
P13	844.90 ± 161.58^{a,b,c}	953.20 ± 139.90^{a,b,c}	828.90 ± 156.74^{a,b,c}	912.40 ± 135.94^a
P14	761.50 ± 135.34^{a,b,c}	938.50 ± 123.64^{a,b,c}	781.20 ± 121.56^{a,b,c}	858.70 ± 104.81^a
P15	690.70 ± 81.73^{a,b,x}	983.60 ± 138.86^{a,b,c,y}	654.50 ± 73.90^{a,b}	735.00 ± 60.93^a

Data were expressed as means ± SEM.
^{x,y}Significant differences in total tibial GP length between 0 and 72 h of incubation in each age group.
^{a,b,c}Significant differences in total tibial GP length between the age groups in each incubation group ($P < 0.05$; 2-way ANOVA).

of the age groups under investigation. The increase in chondrocyte density along the GP zones might have been the major cause of the increase in bone lengthening in the current study. It was established by Williams et al[49] that increases in chondrocyte density, particularly at the proliferating zone of the EGP, significantly affect overall bone growth. The method used for chondrocyte density assessment, as a means of evaluating cellular proliferation along the EGP in this study, was a subjective assessment of cellular proliferation. The gold standard technique currently in use is BrdU immunohistochemical staining using anti BrdU primary antibody, as reported by Mangiavis et al.[50] The BrdU must be injected into the experimental animals 2-4 hours before bone sampling. Nonetheless, recent findings have indicated that BrdU staining has the major limitation of causing tissue damage; this is because the detection of the BrdU in the sampled tissue requires the use of trypsin.[51]

The rate of longitudinal bone growth was reported by Willams et al and Ballock and O'Keefe[28,49] to be dependent on the rate at which the chondrocytes divide in the proliferative zone, the rate at which they enlarge in the hypertrophic zone and the rate at which they synthesize and degrade extracellular matrix substance. In this study, increases in chondrocyte volume were not determined, but it was apparent that the density of the chondrocytes plays a key role in bone elongation. Shapiro et al, Villemure and Stroke, and Srinivas and Shapiro[22,52,53] have reported analyses of bone growth in which the chondrocyte production and their enlargement were determined by the resulted bone growth rate. Their findings also identified the number (pool) of proliferative cells and the ultimate terminal size of hypertrophic chondrocytes as the key parameters of growth plate performance, and they claimed that the rate of chondrocyte division varies less than these two factors, in a given individual.

In summary, our findings demonstrate that ex vivo growth of tibia and metatarsal bone of 7- to 15-day-old rats can be achieved under appropriate physiological conditions. The maximum growth rate during ex vivo culture was seen in tibia of postnatal 10-day-old rats, while the highest growth rate was seen in metatarsal bone of postnatal 15-day-old rats. Histological sectioning of tibial bones from P7-P13 rats can be conveniently carried out without the need for decalcification, while metatarsal bones can be sectioned without need for decalcification at all ages studied (up to P15). The different age groups showed different growth rates and bones continue to grow up to 72 hours ex vivo, with average growth rates of 23.87 ± 0.80% and 40.38 ± 0.95% for tibia and metatarsal bones, respectively. Increases in chondrocytes density along the EGP length appeared to influence bone elongation more than increases in total EGP length. This model should allow direct determination of longitudinal bone growth ex vivo, under normal conditions.

ACKNOWLEDGEMENTS

CONFLICT OF INTEREST

None.

AUTHOR CONTRIBUTIONS

All listed authors have participated in the study and meet the requirements for publication. LMY, NMM and TATI conceived the idea and designed the research; AAA, KOH, MSK, AKA and SMI conducted the research and drafted the initial manuscript. UK analyzed the data and interpreted the results. All authors read and approved the final manuscript draft.

ORCID

Adamu Abdul Abubakar https://orcid.org/0000-0001-8643-4413
Loqman Mohamad Yusof https://orcid.org/0000-0001-9433-4260

REFERENCES

1. Mackie EJ, Tatarczuch L, Mirams M. The skeleton: a multi-functional complex organ: the growth plate chondrocyte and endochondral ossification. *J Endocrinol*. 2011;211:109-121.
2. Tsang KY, Chan D, Cheah KS. Fate of growth plate hypertrophic chondrocytes: death or lineage extension? *Dev Growth Differ*. 2015;57:179-192.
3. Dowthwaite GP, Bishop JC, Redman SN, et al. The surface of articular cartilage contains a progenitor cell population. *J Cell Sci*. 2004;117:889-897.
4. Loqman MY, Bush PG, Farquharson C, Hall AC. Suppression of mammalian bone growth by membrane transport inhibitors. *J Cell Biochem*. 2013;114:658-668.
5. Staines KA, Pollard AS, McGonnell IM, Farquharson C, Pitsillides AA. Cartilage to bone transitions in health and disease. *J Endocrinol*. 2013;219:R1-R12.
6. Sun MM, Beier F. Chondrocyte hypertrophy in skeletal development, growth, and disease. *Birth Defects Res C Embryo Today*. 2014;102:74-82.
7. Studer D, Millan C, Öztürk E, Maniura-Weber K, Zenobi-Wong M. Molecular and biophysical mechanisms regulating hypertrophic differentiation in chondrocytes and mesenchymal stem cells. *Eur Cells Mater*. 2012;24:118-135.
8. Chagin AS, Karimian E, Sundström K, Eriksson E, Sävendahl L. Catch-up growth after dexamethasone withdrawal occurs in cultured postnatal rat metatarsal bones. *J Endocrinol*. 2010;204:21-29.
9. Sun H, Zang W, Zhou B, Xu L, Wu S. DHEA suppresses longitudinal bone growth by acting directly at growth plate through estrogen receptors. *Endocrinology*. 2011;152:1423-1433.
10. Abubakar AA, Noordin MM, Azmi TI, Kaka U, Loqman MY. The use of rats and mice as animal model in ex vivo bone growth and development studies. *Bone Joint Res*. 2016;5:610-618.
11. Loqman MY, Bush PG, Farquharson C, Hall AC. A cell shrinkage artefact in growth plate chondrocytes with common fixative solutions: importance of fixative osmolarity for maintaining morphology. *Eur Cell Mater*. 2010;19:214-227.
12. Marino S, Staines KA, Brown G, Howard-Jones RA, Adamczyk M. Models of ex vivo explant cultures: applications in bone research. *BoneKey Rep*. 2016;5:818.
13. Houston DA, Staines KA, MacRae VE, Farquharson C. Culture of murine embryonic metatarsals: a physiological model of endochondral Ossification. *J Vis Exp*. 2016;118:e54978.

14. Rahman H, Qasim M, Schultze FC, Oellerich M, Asif AR. Fetal calf serum heat inactivation and lipopolysaccharide contamination influence the human T lymphoblast proteome and phosphoproteome. *Proteome Science*. 2011;9:71.

15. Mårtensson K, Chrysis D, Sävendahl L. Interleukin-1β and TNF-α act in synergy to inhibit longitudinal growth in fetal rat metatarsal bones. *J Bone Mine Res*. 2004;19:1805-1812.

16. Dettmeyer RB. Staining Techniques and Microscopy. In: Dettmeyer RB, ed. *Forensic histopathology fundamental and perspectives*. 1st edn. Berlin, Heidelberg: Springer-Verlang; 2011:17-35.

17. Pastoureau PC, Hunziker EB, Pelletier JP. Cartilage, bone and synovial histomorphometry in animal models of osteoarthritis. *Osteoarthritis Cartilage*. 2010;18:S106-S112.

18. Schmitz N, Laverty S, Kraus VB, Aigner T. Basic methods in histopathology of joint tissues. *Osteoarthritis Cartilage*. 2010;18:S113-S116.

19. Alvarez J, Balbín M, Santos F, Fernández M, Ferrando S, López JM. Different bone growth rates are associated with changes in the expression pattern of types II and X collagens and collagenase 3 in proximal growth plates of the rat tibia. *J Bone Mine Res*. 2000;15:82-94.

20. Wilsman NJ, Bernardini ES, Leiferman E, Noonan K, Farnum CE. Age and pattern of the onset of differential growth among growth plates in rats. *J Orthop Res*. 2008;26:1457-1465.

21. Bush PG, Pritchard M, Loqman MY, Damron TA, Hall AC. A key role for membrane transporter NKCC1 in mediating chondrocyte volume increase in the mammalian growth plate. *J Bone Mine Res*. 2010;25:1594-1603.

22. Shapiro IM, Adams CS, Freeman T, Srinivas V. Fate of the hypertrophic chondrocyte: microenvironmental perspectives on apoptosisand survival in the epiphyseal growth plate. *Birth Defects Res C Embryo Today*. 2005;75:330-339.

23. Amini S, Veilleux D, Villemure I. Three-dimensional in situ zonal morphology of viable growth plate chondrocytes: a confocal microscopy study. *J Orthop Res*. 2010;29:710-717.

24. Tivesten A, Movérare-Skrtic S, Chagin A, et al. Additive protective effects of estrogen and androgen treatment on trabecular bone in ovariectomized rats. *J Bone Mine Res*. 2004;19:1833-1839.

25. Weise M, De-Levi S, Barnes KM, Gafni RI, Abad V, Baron J. Effects of estrogen on growth plate senescence and epiphyseal fusion. *Pro Natl Acad Sci U S A*. 2001;98:6871-6876.

26. Gruber HE, Ingram JA. Basic Staining Techniques for Cartilage Sections. In: An YH, Martin KL, eds. *Handbook of histology methods for bone and cartilage*. Totowa, NJ: Humana Press; 2003:287-293.

27. Dobie R, Ahmed SF, Staines KA, et al. Increased linear bone growth by GH in the absence of SOCS2 is independent of IGF-1. *J Cell Physiol*. 2015;230:2796-2806.

28. Ballock RT, O'Keefe RJ. Physiology and pathophysiology of the growth plate. *Birth Defects Res C Embryo Today*. 2003;69:123-143.

29. Chung UI. Essential role of hypertrophic chondrocytes in endochonral ossification in bone development. *Endocr J*. 2004;51:19-24.

30. Mackie EJ, Ahmed YA, Tatarczuch L, Chen KS, Mirams M. Endochondral ossification: how cartilage is converted into bone in the developing skeleton. *Int J Biochem Cell Biol*. 2008;40:46-62.

31. Rolian C. Developmental basis of limb length in rodents: evidence for multiple divisions of labor in mechanisms of endochondral bone growth. *Evol Dev*. 2008;10:15-28.

32. Walzer SM, Cetin E, Grubl-Barabas R, et al. Vascularization of primary and secondary ossification centers in the human growth plate. *BMC Dev Biol*. 2014;14:36.

33. Enishi T, Yukata K, Takahashi M, Sato R, Sairyo K, Yasui N. Hypertrophic chondrocytes in the rabbit growth plate can proliferate and differentiate into osteogenic cells when capillary invasion is interposed by a membrane filter. *PLoS ONE*. 2014;9:e104638.

34. Kronenberg HM. Developmental regulation of the growth plate. *Nature*. 2003;423:332-336.

35. Yang L, Tsang KY, Tang HC, Chan D, Cheah KS. Hypertrophic chondrocytes can become osteoblasts and osteocytes in endochondral bone formation. *Proc Natl Acad Sci U S A*. 2014;111:12097-12102.

36. de Crombrugghe B, Lefebvre V, Nakashima K. Regulatory mechanisms in the pathways of cartilage and bone formation. *Cur Opin Cell Biol*. 2001;13:721-727.

37. Farnum CE, Lee R, O'Hara K, Urban JP. Volume increase in growth plate chondrocytes during hypertrophy: the contribution of organic osmolytes. *Bone*. 2002;30:574-581.

38. von Pfeil DJ, DeCamp CE. The epiphyseal plate: physiology, anatomy and trauma. *Compend Contin Educ Vet*. 2009;31:E1-E11.

39. Nilsson O, Baron J. Fundamental limits on longitudinalbone growth: growth plate senescenceand epiphyseal fusion. *Trends Endocrinol Metab*. 2004;15:371-374.

40. Cooper KL, Oh S, Sung Y, Dasari RR, Kirschner MW, Tabin CJ. Multiple phases of chondrocyte enlargement underlie differences in skeletal proportions. *Nature*. 2013;495:375-378.

41. Mohammad KS, Chirgwin JM, Guise TA. Assessing new bone formation in neonatal calvarial organ culture. *Methods Mol Biol*. 2008;455:37-50.

42. Martin EA, Ritman EL, Turner RT. Time course of epiphyseal growth plate fusion in rat tibiae. *Bone*. 2003;32:261-267.

43. Nilsson O, Marino R, De Luca F, Phillip M, Baron J. Endocrine regulation of the growth plate. *Horm Res*. 2005;64:157-165.

44. Shim KS. Pubertal growth and epiphyseal fusion. *Ann Pediatr Endocrinol Metab*. 2015;20:8-12.

45. Wilsman NJ, Farnum CE, Green EM, Lieferman EM, Clayton MK. Cell cycle analysis of proliferative zone chondrocytes in growth plates elongating at different rates. *J Orthop Res*. 1996;14:562-572.

46. Gkiatas L, Lykissas M, Kostas-Agnantis L, Korompilias A, Batistatou A, Beris A. Factors affecting bone growth. *Am J Orthop (Belle Mead NJ)*. 2015;44:61-67.

47. Locatelli V, Bianchi VE. Effect of GH/IGF-1 on bone metabolism and osteoporsosis. *Int J Endocrinol*. 2014;2014:235060.

48. Giustina A, Mazziotti G, Canalis E. Growth hormone, insulin-Like growth factors, and the skeleton. *Endocr Rev*. 2008;29:535-559.

49. Williams JL, Do PD, Eick JD, Schmidt TL. Tensile properties of the physis vary with anatomic location, thickness, strain rate and age. *J Orthop Res*. 2001;19:1043-1048.

50. Mangiavini L, Merceron C, Schipani E. Analysis of mouse growth plate development. *Curr Protoc Mouse Biol*. 2017;6:67-130.

51. Salic A, Mitchison TJ. A chemical method for fast and sensitive detection of DNA synthesis in vivo. *Proc Natl Acad Sci U S A*. 2008;105:2415-2420.

52. Srinivas V, Shapiro IM. The Epiphyseal Growth Plate: the Engine That Drives Bone Elongation. In: Preedy VR, ed. *Handbook of growth and growth monitoring in health and disease*. New York, NY: Springer; 2012:1331-1349.

53. Villemure I, Stokes IA. Growth plate mechanics and mechanobiology. A survey of present understanding. *J Biomech*. 2009;42:1793-1803.